A simple approach to rGO deposition on aluminium alloys for corrosion and wear protection

Stefano Caporali* and Nicola Calisi

Department of Industrial Engineering, DIEF, University of Florence, Florence, Italy, and Consorzio INSTM, Florence, Italy
stefano.caporali@unifi.it

** Corresponding author.*

Aluminium and its alloys rely on a thin native oxide film for corrosion resistance; however, in chloride-containing environments this passive layer is prone to localized breakdown and pitting corrosion. Reduced graphene oxide (rGO) has emerged as a promising material for aluminium corrosion protection due to its high aspect ratio, excellent impermeability, chemical and mechanical stability. When used as a coating component or nanofiller in paints rGO significantly enhances barrier properties. In this work rGO was obtained by simple reduction with L-ascorbic acid from GO solution and its direct application on commercial aluminium alloys, commonly used for structural applications, is investigated as an anti-corrosion and anti-wear coating by means of electrochemical techniques and tribology. The results support the effectiveness and suitability of such simple, inexpensive, and environmentally friendly treatment, capable to enhance the stability of the surface passive layer.

Aluminium alloys are indispensable structural materials in modern engineering due to their low density, high specific strength, and good formability. They are widely applied in aerospace, marine and transportation sectors, and emerging energy technologies. The corrosion resistance of aluminium originates from the rapid formation of a thin, adherent oxide film (Al_2O_3) that passivates the surface under neutral and mildly alkaline conditions [1, 2]. Despite this natural passivity, aluminium alloys are highly susceptible to localized corrosion in the presence of aggressive anions, particularly chloride ions [3]. Pitting corrosion represents the most critical degradation mechanism, as it can initiate at microscopic defects, intermetallic particles, or inclusions and propagate rapidly with limited macroscopic warning. Once the passive film breaks down, localized dissolution is sustained by autocatalytic mechanisms involving local acidification and chloride enrichment.
Historically, chromate-based conversion coatings have provided excellent corrosion protection for aluminium alloys. However, due to the toxicity and carcinogenicity of hexavalent chromium compounds, increasingly stringent environmental regulations have driven intense research into chromate-free alternatives. In this context, nanomaterial-enabled coatings—especially those based on graphene derivatives—have attracted significant attention [4-6]. Among graphene-based materials, reduced graphene oxide (rGO) offers a unique combination of properties: high impermeability comparable to graphene, residual functional groups that improve dispersion and adhesion, and scalable synthesis routes [7]. Generally, the conversion from GO to r-GO requires a reducing agents [8-9] or thermal treatment [10-14], or even bacterial methods [15]. However, in order to propose a simple and easily scalable process for industrial applications, several aspects need to be accurately taken into consideration, the most relevant of which are the use of water-based treatments and the use of inexpensive and benign reducing agents. Based on these concerns many commonly used chemical reductants, such as hydrazine, hydrazine hydrate, and NaBH4 need to be avoided. Green reductants, such as L-ascorbic acid (L-aa) [16-18], L-cysteine [19] and even various plant extracts [20-22], have been proposed. Despite inherent limitations—such as reduced deposition efficiency arising from the formation of graphene agglomerates that do not participate in film growth, and the requirement for moderately elevated processing temperatures (>60 °C), which restrict applicability to thermally sensitive substrates—this method remains the most viable and scalable approach for the deposition of rGO coatings on metallic substrates [23], including in industrial and artisanal manufacturing contexts.

Experimental procedures

Samples preparation

Metallic substrates were prepared from commercially available bars of AA5754 and AA6068 aluminium alloys [their chemical composition, as determined by XRF-WDS (Rigaku ZSX Primus II), are depicted in **Table 1**] as 1 mm thick and 50 mm diameter tokens. The samples were than grinded with emery paper down to 1200 grit, rinsed in distilled water, acetone and then air dried letting the spontaneous oxidation film to be formed on the sample surface.

Alloy designation	Composition (Wt%)									
	Si	Fe	Mn	Mg	Cu	Zn	Cr	Ti	V	Al
AA5754	0.35	0.26	0.40	3.2	0.10	0.18	0.25	0.1	0.01	balance
AA6068	0.40	0.34	0.57	1.1	0.10	0.20	0.30	0.1	n.d.	balance

Table 1: Designation, chemical composition (Wt%) and of the aluminium alloys tested.

Reduced graphene oxide (rGO) coatings were deposited on the sample surface by immersing the metallic tokens in an aqueous solution prepared by diluting a commercial graphene oxide (GO) dispersion (0.4 wt%, Goodfellow) with Milli-Q water to a final GO concentration of 0.1 mg/mL^{-1}. L-ascorbic acid (99%, Merck) was added as a reducing agent in the amount of 4 g/L^{-1}. Solution containing the immersed samples was then heated at 80 °C under continuous stirring (≈600 rpm) for 2 h. During the process, the solution colour changed from grey to brownish and a rGO film is deposited on the solid surfaces in owe to the reduced solubility of rGO respect to the GO. As side by-products some colloidal graphene agglomerates appeared. Following the treatment, the samples were retrieved from the solution, gently rinsed with Milli-Q water, air-dried, and then subjected to subsequent testing and characterization. Visual investigation of the samples so produced was obtained by means of digital magnifier (OCULUX Macro Zoom, Microconsult).

Electrochemical tests

The potential effect of rGO as an anticorrosive coating was assessed by electrochemical techniques. A computer controlled potentiostat (Autolab, Metrohm) controlled via Intello electrochemical software (vers. 2.1) and a three-electrode corrosion cell (EG&G Parr Flat cell) constituted the electrochemical set-up. 1 cm^2 is the exposed area of the working electrode while a platinum grid and a saturated calomel electrode (SCE) constituted counter and reference electrodes, respectively. Electrochemical tests were carried out in aerated 5% NaCl solution at room temperature. Prior to each measurement, open-circuit potential (OCP) was recorded until a stable potential was reached (about 1 hour), then EIS and potentiodynamic polarization (PDP) measurements were performed. EIS measurements were carried out with an AC amplitude of 10 mV at open circuit potential in the frequency range 100 kHz to 1000 mHz while, successively to the EIS measurement PDP curves were registered at scanning rate of 0.1667mV/s from -0.9V to -0.2V vs SCE in the anodic direction. The inhibition efficiency (IE) of the rGO coating was calculated accordingly to the following equation (1)

$$IE\% = 100 \times \frac{icorr,ref - icorr,rGO}{icorr,ref} \quad (1)$$

Where:
IE = inhibition efficiency; i_{corr}, ref= corrosion current of the untreated aluminium sample; i_{corr}, rGO = corrosion current of the rGO treated sample.

Among graphene-based materials, reduced graphene oxide (rGO) offers a unique combination of properties: high impermeability comparable to graphene, residual functional groups that improve dispersion and adhesion, and scalable synthesis routes.

Tribological tests

The coefficient of friction (COF) was determined using a ball-on-disk tribometer (POD 4.0, Ducom Instruments, India), in which a stationary spherical ball (10 mm diameter, in our case) was brought into sliding contact with a rotating disk specimen under controlled conditions applying a constant normal load throughout the test. During testing, that was carried at room temperature, the friction force generated at the ball–disk interface was continuously measured, and the COF was calculated as the ratio of the measured friction force to the applied normal load (4 N) as function of the sliding distance. **Figure 1** depicts a scheme of test. Three replicate tests were carried out for each specimen, and at the end of the test, the worn samples were observed by SEM microscopy (Hitachi, SU3800, filament electron source) operating at 15keV and 16.3mm working distance.

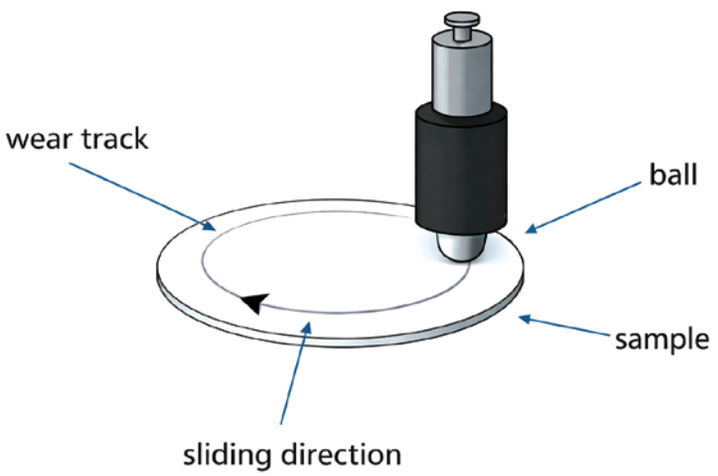

Figure 1 - Sketch of the ball-on-disk principle. The wear test was performed with a 10 mm diameter ball applying a normal load of 4 N.

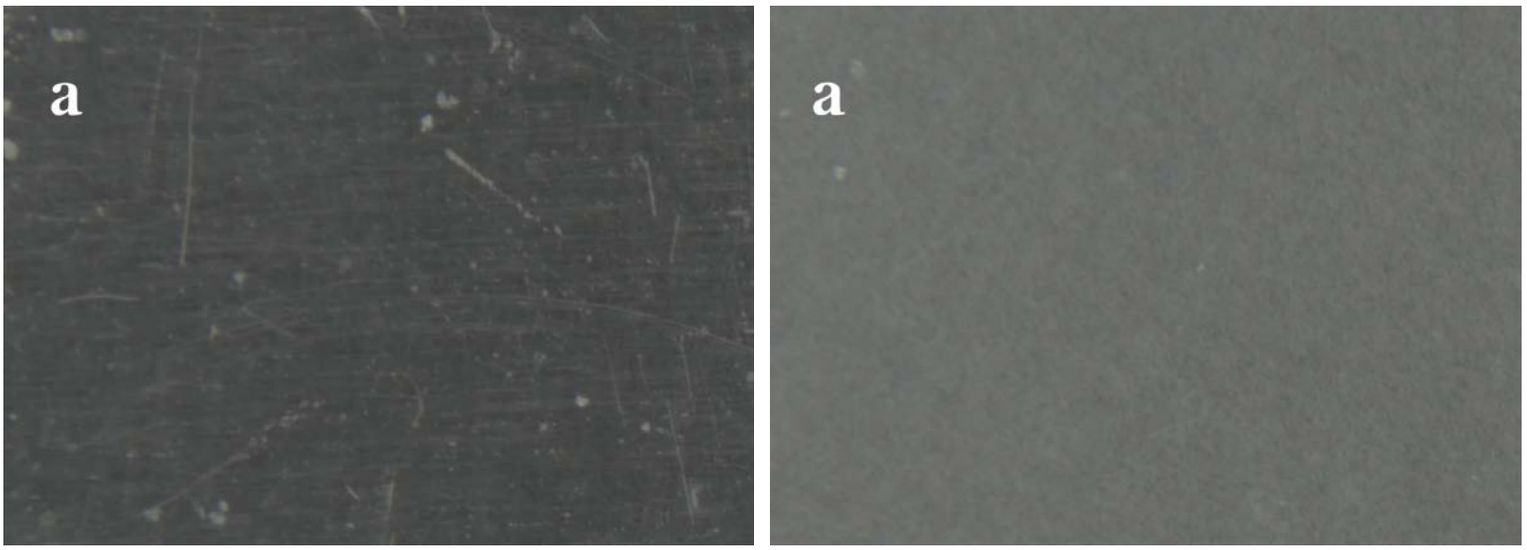

Figure 2 - Digital macro images of the sample AA5754 before (a) and after (b) the deposition of rGO coating (field of view 3mm x2mm).

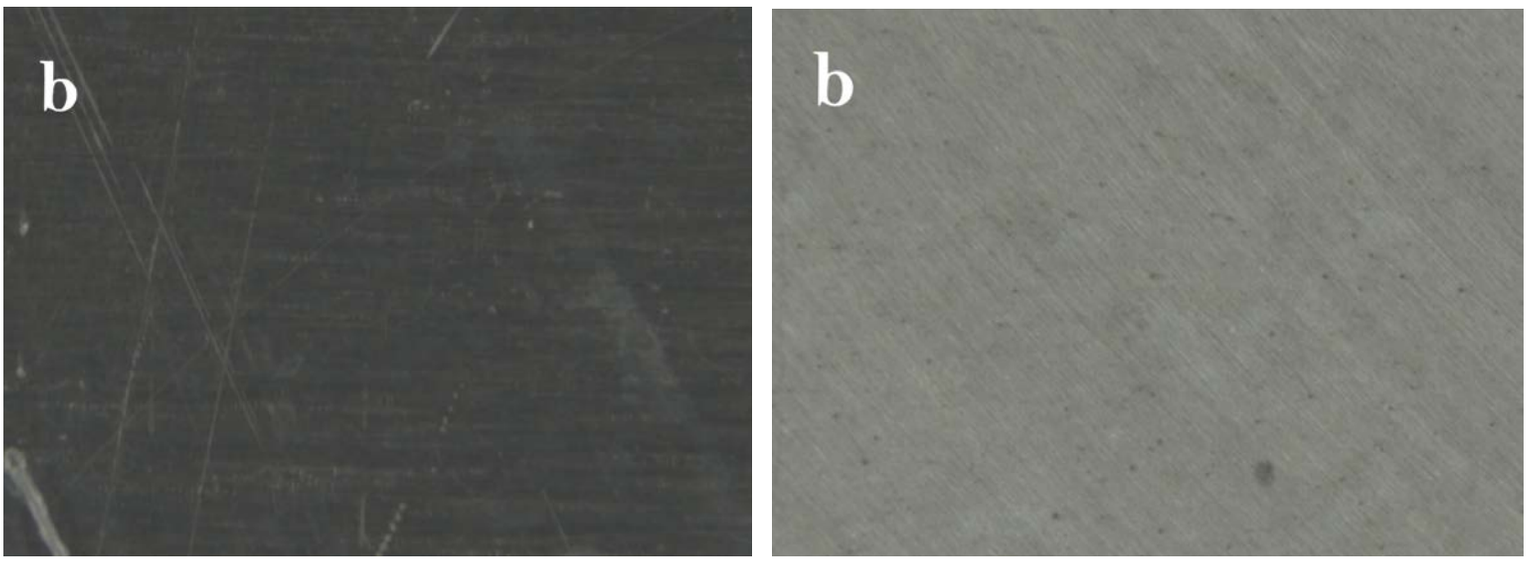

Figure 3 - Digital macro images of the sample AA6068 before (a) and after (b) the treatment with rGO (field of view 3mm x2mm).

Results

Sample preparation

The detailed physical characterization of the rGO layer obtained via GO reduction with L-ascorbic acid is reported in literature [23-25], in our case the successfully formation of rGO film was cheked by FTIR measurements (not reported here) and visual investigation. Representative images of the sample surface before and after the deposition of rGO are depicted in **Figure 2** (AA5754 alloy) and **Figure 3** (AA6068 alloy). For both aluminium alloys, no detectable changes in surface morphology were observed after the treatment; however, the treated samples exhibited a slight, but clearly visible, shift in colour towards a more brownish hue.

Electrochemical corrosion tests

PDP curves are shown in **Figure 4**, and values of Ecorr and icorr obtained by the tangent extrapolation method are displayed in **Table 2**. Despite the Ecorr values remain almost unaffected by the rGO treatment the icorr values showed a clear decrease pointing out a corrosion reduction with inhibition efficiency (IE%) values respectively of 82% for AA6068 and 84% for AA5754.
The corrosion protection performance of the rGO coating on Al alloys was investigated by electrochemical impedance spectroscopy (EIS). The Nyquist plots, and the corresponding equivalent electrical circuit, are presented in **Figure 5**.

Alloy	E_{corr} (V vs SCE)	i_{corr} (µA/cm²)	E_{corr} (V vs SCE)	i_{corr} (µA/m²)	inhibition efficiency (IE, %)
	untreated		+ rGO		
AA5754	-0.73± 0.01	1.1 ± 0.1	-0.72± 0.01	0.2 ± 0.1	84
AA6068	-0.72 ± 0.01	5.7 ± 0.1	-0.71 ± 0.01	0.61 ± 0.1	82

Table 2: Electrochemical corrosion values obtained from PDP curves.

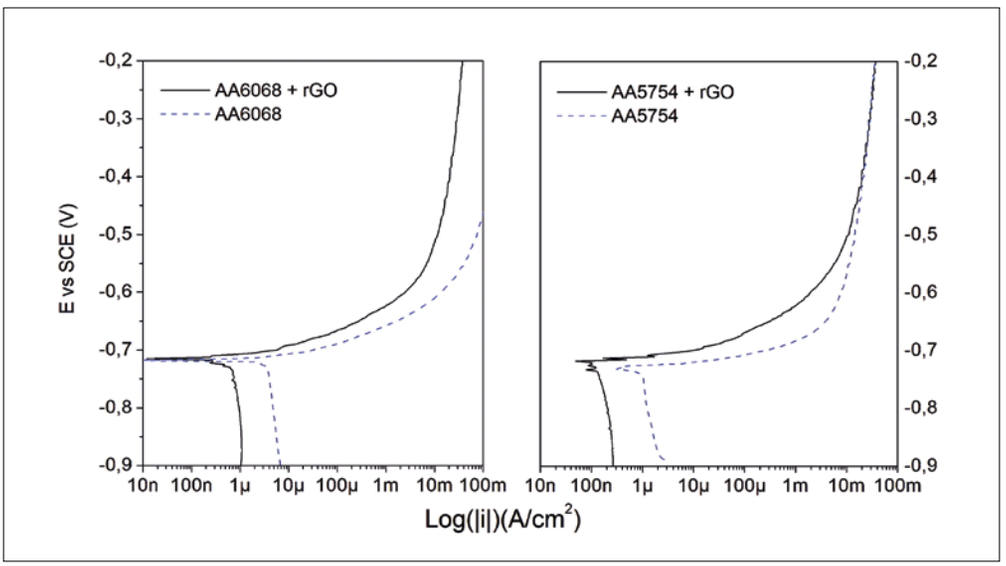

Figure 4 - PDP curves of uncoated (dashed curves) and rGO-coated (solid curves) Al samples recorded in aerated 5% NaCl. Coated samples show a clear decrease in i_{corr} values, compatible with an inhibition of the corrosion process.

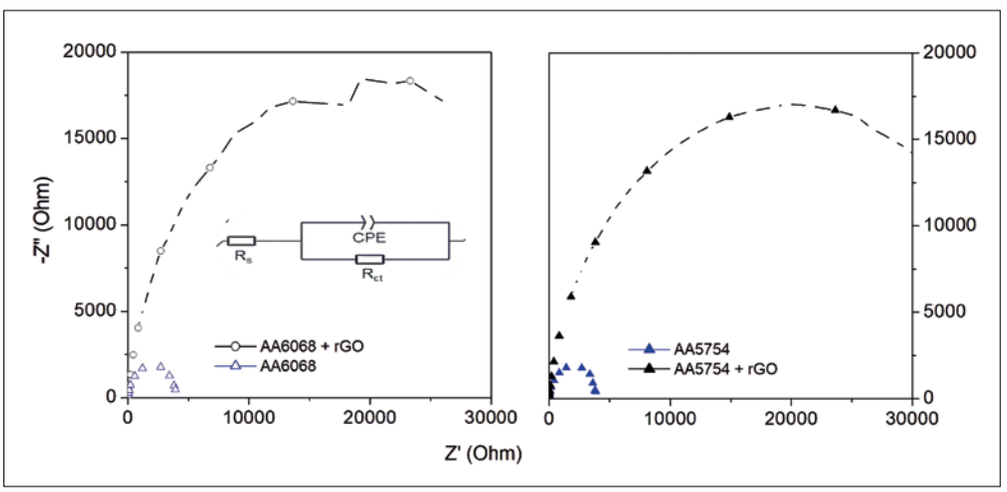

Figure 5 - Nyquist plots for uncoated and coated Al samples. The inset displays the proposed circuit equivalent.

The equivalent circuit consists of the solution resistance (Rs), the charge transfer resistance (Rct), and a constant phase element (CPE). The Nyquist plots of both coated and uncoated samples exhibit a typical depressed semicircular shape in the high-frequency region. Notably, the diameter of the semicircle for the rGO-coated samples is significantly larger than that of the uncoated sample. This increase indicates a higher charge transfer resistance (Rct), which is associated with enhanced corrosion resistance of the coated aluminium samples.

Wear tests

To better elucidate the role of rGO, the wear behaviour of treated and untreated samples was investigated using ball-on-disk tribometry. **Figure 6** depicts the coefficient of friction (COF) as a function of sliding distance (m). The red curves correspond the untreated samples, whereas the blue curves represent the rGO-treated samples. After rGO treatment, both alloys exhibit a significant stabilization and reduction of COF values. **Figures 7 and 8** display the SEM images of the wear surfaces for the treated and untreated samples. The wear scars on both the untreated alloys are characterized by their extensive width and roughness, accompanied by a plethora of debris. Additionally, the friction ball associated with the untreated sample displays a considerable amount of wear debris (not displayed here), showing the presence of severe adhesion wear and justifying the high variability of COF. Nevertheless, the samples treated with rGO exhibited much smaller wear track, consistent with reduced COF and almost none wear debris.

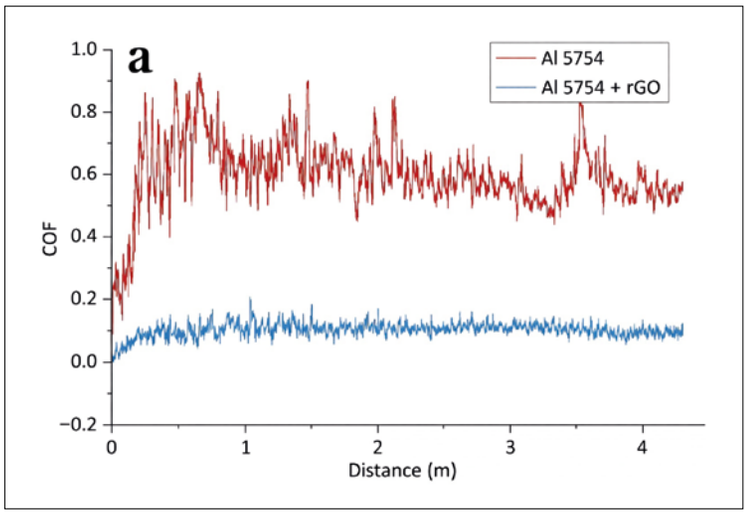

Figure 6 - The coefficient of friction (COF) as a function of sliding distance (m) for untreated (a) and rGO – treated (b) samples.

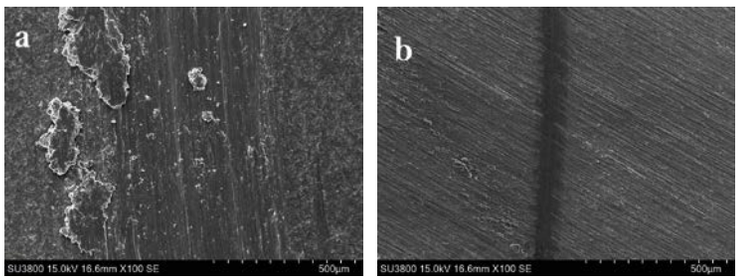

Figure 7 - SEM micrographs of wear traces on AA5754: (a) Untreated sample, (b) rGO treated sample. Same magnification for the two samples, scale bar in the picture.

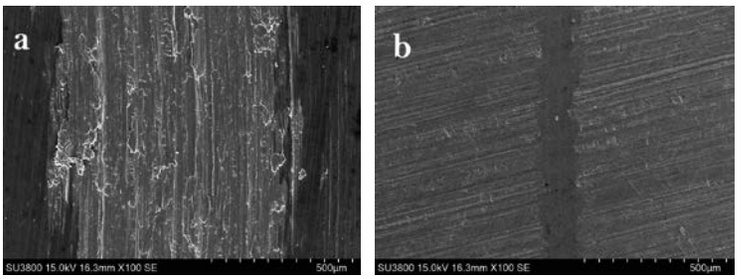

Figure 8 - SEM micrographs of wear traces on AA6068: (a) Untreated sample, (b) rGO treated sample. Same magnification for the two samples, scale bar in the picture.

Discussions

It is well known that rGO obtained by partial reduction of GO via chemical reduction in aqueous environment, retains residual oxygen-containing functional groups that enhance adhesion capability towards the oxide layer present on the surface of air-exposed aluminium items. [26]. After deposition of rGO layer the colour of the samples turns towards a more brownish hue but, from the electrochemical point of view no significative change in the OCP and Ecorr, respect to the untreated samples were observed (Figure 4). Such electrochemical data asses that the rGO layer is not in direct contact with metallic surfaces, avoiding the potential galvanic coupling which could increase the corrosion rate. [27,28]. That is probably due to the partial surface coverage by rGO layer and the absence of direct contact of the rGO layer with metal parts.

The electrochemical data asses that the rGO layer is not in direct contact with metallic surfaces, avoiding the potential galvanic coupling which could increase the corrosion rate. That is probably due to the partial surface coverage by rGO layer and the absence of direct contact of the rGO layer with metal parts.

Nevertheless, the presence of such film effectively reduces the corrosion rate in mild NaCl bearing environments, limiting the icorr of about 1 order of magnitude (table 2) with respect to the untreated samples. The inhibition effect player by rGO layer is reasonably attributable to the increased charge transfer resistance (Rct) as highlighted by EIS measurements (Figure 5). That is consistent with a reducing permeation of water, oxygen, and chloride ions as proposed in previous works [29, 30] and is attributed to the near-impermeability to gases and liquids of graphene-like materials. Furthermore, the increased hydrophobicity and the lubricating effect played by the rGO layer, as demonstrated by the wear tests (Figure 6), may further inhibit the retention of aqueous solution at the surface or within the pores of the oxide layer, effectively enhancing the barrier effect, which is widely recognized as the predominant corrosion protection mechanism of rGO-based coatings.

Conclusions

A reduced graphene oxide (rGO) layer was successfully deposited onto commercial grade aluminium alloys by the simple reduction of GO aqueous solutions using L-ascorbic acid. The capability of the film, so generated, to improve the anticorrosion characteristics of two different aluminium alloys (namely AA5754 and AA6068) widely used for structural applications was successfully tested in aerated NaCl aqueous solution via electrochemical test. Potentiodynamic polarization measurements demonstrate that rGO coatings does not significatively affects the corrosion potential (Ecorr) but indeed reduce the corrosion rate of about 84% and 82% for AA5754 and AA6068, respectively. EIS measurement confirms this behaviour indicating a strong increment of the polarization resistance respect to the untreated samples. On the other hand, wear tests conducted using ball-on-disk measurements highlighted that the rGO layer plays a beneficial role in reducing the coefficient of friction. In treated samples the scar traces resulted much smaller and a reduced presence of debris was observed. These effects are reasonably attributable to the formation of an almost continuous layer of graphene-like material, strongly adhering to the substrate, which impair the direct contact between the friction ball and the surface of the sample thereby reducing wear. The observed corrosion inhibition effect can be also due to the capability of rGO layer to impair the penetration of aggressive agent (mainly water and chloride ions) inside the pores and cracks naturally present on the surface.

This study presents a relatively simple and cost-effective approach to improving the corrosion and wear resistance of bare aluminium alloys for practical applications in mild ambient environments, while preserving their aesthetic appearance. Although the enhancement in corrosion resistance is lower than that provided by conventional chromate-based conversion coating or anodizing treatments, the simplicity of the process and the low cost and low toxicity of the reagents make this environmentally benign method well suited for large-scale industrial implementation.

Acknowledgements

The authors acknowledge financial support from the Italian Ministry for enterprise and made in Italy (MIMIT) for partially supporting this research through the project: "Studio di applicazioni industriali innovative del graphene" (Acronim: GRAFENEX) funded within the call:"Accordi per l'Innovazione" (D.M. MiSE 31/12/2021).

References

[1] W.A. Badawy, F.M. Al-Kharafi, A.S. El-Azab, "Electrochemical behaviour and corrosion inhibition of Al, Al-6061 and Al-Cu in neutral aqueous solutions", Corros. Sci. vol 41, pp. 709–727, 1999

[2] R. G. Kelly, et al., "Passivity and localized corrosion", in "Electrochemical techniques in corrosion science and engineering". Marcel Dekker inc., 2002, 55-123.

[3] R. C. Newman, "Local chemistry considerations in the tunnelling corrosion of aluminium" Corros Sci. vol 37, 3, pp. 527-533, 1995

[4] S.J. Richard Prabakar, Y.-H. Hwang, E.G. Bae, D.K. Lee, M. Pyo, "Graphene oxideas a corrosion inhibitor for the aluminum current collector in lithium ionbatteries", Carbon vol 52, pp 128–136, 2013

[5] S. Chen, L. Brown, M. Levendorf, W. Cai, S.-Y. Ju, J. Edgeworth, X. Li, C.W.Magnuson, A. Velamakanni, R.D. Piner, J. Kang, J. Park, R.S. Ruoff, "OxidationResistance of Graphene-Coated Cu and Cu/Ni Alloy", ACS Nano 5, pp 1321–1327, 2011

[6] A.S. Kousalya, A. Kumar, R. Paul, D. Zemlyanov, T.S. Fisher, "Graphene: an effective oxidation barrier coating for liquid and two-phase cooling systems", Corros. Sci. 69, 5–10, 2013

[7] Y. Liu, J. Zhang, S. Li, Y. Wang, Z. Han, L. Ren, "Fabrication of a superhydrophobic graphene surface with excellent mechanical abrasion and corrosion resistance on an aluminum alloy substrate", RSC Adv. 4, pp 45389–45396, 2014

[8] C.K. Chua, M. Pumera, "Chemical reduction of graphene oxide: A synthetic chemistry viewpoint. Chem. Soc. Rev. 43, pp 291–312, 2014

[9] C.K. Chua, M. Pumera, "The reduction of graphene oxide with hydrazine: Elucidating its reductive capability based on a reaction-model approach" Chem. Commun. 52, pp 72–75, 2016

[10] R. Jakhar, J.E. Yap, R. Joshib, "Microwave reduction of graphene oxide". Carbon 170, pp 277–293, 2020

[11] V.V. Chaban, O.V. Prezhdo, "Microwave reduction of graphene oxide rationalized by reactive molecular dynamics". Nanoscale, 9, pp 4024–4033, 2017

[12] O.M. Slobodian, P.M. Lytvyn, A.S. Nikolenko, V.M. Naseka, O.Y. Khyzhun, A.V. Vasin,S.V. Sevostianov, A.N. Nazarov, "Low-Temperature Reduction of Graphene Oxide: Electrical Conductance and Scanning Kelvin Probe Force Microscopy". Nanoscale Res. Lett. 13, 139, 2018

[13] W. Gao, N. Singh, L. Song, Z. Liu,A.L. Reddy, L. Ci, R. Vajtai, Q. Zhang, B. Wei, P.M. Ajayan, "Direct laser writing of micro-supercapacitors on hydrated graphite oxide films" Nat. Nanotechnol. 6, pp 496–500, 2011

[14] A. Longo, R. Verrucchi, L. Aversa, R. Tatti, A. Ambrosio, E. Orabona, U. Coscia, G. Carotenuto, P. Maddalena, "Graphene oxide prepared by graphene nanoplatelets and reduced by laser treatment" Nanotecnology, 28, pp 224002–224008, 2017

[15] G. Utkan, T. Öztürk, Ö. Duygulu, E. Tahtasakal, A.A. Denizci, "Microbial Reduction of Graphene Oxide by Lactobacillus Plantarum" Int. J. Nanosci. Nanotechnol. 15, pp 127–136, 2019.

[16] M.J. Fernández-Merino, L. Guardia, J.L. Paredes, S. Villar-Rodil, P. Solís-Fernández, A. Martínez-Alonso, J.M.D. Tascón, "Vitamin C is an ideal substitute for hydrazine in the reduction of graphene oxide suspensions." J. Phys. Chem. C, 214, pp 6426–6432, 2010

[17] A.T. Habte,D.W. Ayele, "Synthesis and Characterization of Reduced Graphene Oxide (rGO) Started from Graphene Oxide (GO) Using the Tour Method with Different Parameters" Adv. Mater. Sci. Eng. 15, 5058163, 2019

[18] J. Liu, L. Liu, X. Wu, X. Zhang, T. Li, "Environmentally friendly synthesis of graphene–silver composites with surface-enhanced Raman scattering and antibacterial activity via reduction with l-ascorbic acid/water vapor" New J. Chem. 39, pp 5272–5281, 2015

[19] A.O.E. Abdelhalim, V.V. Sharoyko, A.A. Meshcheriakov, S.D. Martynova, S.V. Ageev, G.O. Iurev, H.A. Mulla, A.V. Petrov, I.L. Solovstova, L.V. Vasina, "Reduction and functionalisation of graphene oxide with L-cysteine: Synthesis, characterization and biocompatibility" Nanomed. Nanotechnol. Biol. Med. 29, 102284, 2020

[20] Y. Wang, Z. Shi, J.Yin, "Facile Synthesis of Soluble Graphene via a Green Reduction of Graphene Oxide in Tea Solution and Its Biocomposites." ACS Appl. Mater. Interfaces 3, pp 1127–1133, 2011

[21] E. Vatandosta, S. Azade Ghorbani-Hasan, F. Chekin, S.N. Raeisi, S.-A. Shahidi "Green tea extract assisted green synthesis of reduced graphene oxide: Application for highly sensitive electrochemical detection of sunset yellow in food products" Food Chem. X 6, 100085, 2020

[22] B.Z. Kurt, Z. Durmus, E. Sevgi, "In situ reduction of graphene oxide by different plant extracts as a green catalyst for selective hydrogenation of nitroarenes." Int. J. Hydrog. Energy 44, pp 26322–26337, 2019

[23] M. Palomba, G. Carotenuto, A. Longo, "A Brief Review: The Use of L-Ascorbic Acid as a Green Reducing Agent of Graphene Oxide". Materials 15, 6456, 2022

[24] A. Kreta, I. Jerman, M. Bele, A.K. Surca, M. Gaberš˘cek, I. Muševi˘c, "Nanoscopic Characterization of Reduced Graphene Oxide for Anticorrosion Coating of AA2024". Eng. Proc. 87, 82, 2025

[25] K.-O. Hülya, "Evaluation of morphological, structural, thermal, electrical, and chemical composition properties of graphene oxide, and reduced graphene oxide obtained by sequential reduction methods", Carbon Trends, Vol 17, 100429, 2024

[26] S. Pei, H.-M. Cheng, "The reduction of graphene oxide". Carbon 50, pp 3210–3228, 2012

[27] M. Schriver, W. Regan, W.J. Gannett, A.M. Zaniewski, M.F. Crommie, A. Zettl, "Graphene as a long-term metal oxidation barrier". ACS Nano 7, pp 5763–5768, 2013

[28] C. Healy, F. Yu, J.G. Lozano, M.P. Ryan, P.E. McHugh, T. McNally, "Graphene and graphene oxide for corrosion protection of metals". Corros. Mater. Degrad. 1, pp 127–150, 2020

[29] J.S. Bunch, S.S. Verbridge, J.S. Alden, A.M. van der Zande, J.M. Parpia, H.G. Craighead, P.L. McEuen, "Impermeable atomic membranes from graphene sheets". Nano Lett. 8, pp 2458–2462, 2008

[30] B.P. Singh, S. Nayak, K.K. Nanda, S. Bhattacharjee, L. Besra, "Graphene-based materials and their composites: A review on production, characterization and applications". Prog. Mater. Sci. 56, pp 1178–1271, 2013